Materials Today Communications 36 (2023) 106602

Contents lists available at ScienceDirect

Materials Today Communications

journal homepage: www.elsevier.com/locate/mtcomm

# Chemical composition, particle geometry, and micro-mechanical strength of barley husks, oat husks, and wheat bran as alternative raw materials for particleboards

Nicolas Neitzel [a], Michaela Eder [b], Reza Hosseinpourpia [a,c], Thomas Walther [d], Stergios Adamopoulos [e,*]

[a] Linnaeus University, Department of Forestry and Wood Technology, Växjö 35195, Sweden
[b] Max Planck Institute of Colloids and Interfaces, Department of Biomaterials, Research Campus Golm, Potsdam 14424, Germany
[c] College of Forest Resources and Environmental Science, Michigan Technological University, Houghton, MI 49931, United States
[d] IKEA Industry AB, Skrivaregatan 5, Malmö 21532, Sweden
[e] Swedish University of Agricultural Sciences, Department of Forest Biomaterials and Technology, Uppsala 75007, Sweden

ARTICLE INFO

*Keywords:*
Agro-industry residues
Chemical composition
Particle geometry
SEM
X-ray microcomputed tomography
Microtensile strength

ABSTRACT

Particleboards are used worldwide in various industry segments, like construction and furniture production. Nevertheless, increase in wood prices and logistical challenges urge the particleboard industry to find alternative raw materials. By-products and residues from the agricultural and food industries could offer possibilities for material sourcing at a local level. This study aimed to investigate the chemical composition, particle geometry, anatomical structure, and microtensile characteristics of such material, specifically barley husks (BH), oat husks (OH), and wheat bran (WB). BH and OH were found to have comparable hemicelluloses and lignin contents to industrial wood chips but contained more ash. WB was rich in extractives and showed high buffering capacity. Light microscopy and microcomputed tomography revealed details of leaf structure for BH and OH as well as the multi-layer structure of WB. The ultimate microtensile strength of BH, various OH samples, and WB were respectively 2.77 GPa, 0.84–2.42 GPa, and 1.45 GPa. The results indicated that the studied materials could have potential uses as furnish materials in non-load bearing particleboards, where thermal or acoustic insulation properties are desirable.

## 1. Introduction

Wood composites are important materials for construction, shipbuilding, design elements, furniture production, and other sectors. During the last two decades, the global production volume of particleboards, which represents a major product segment of this sector, has increased by 70% [20,59]. This indicates the escalated pressure on the forest as the main supplier of raw materials. According to the European Union Biodiversity Strategy for 2030 and the United Nations Sustainable Development Goals, biodiversity, the quantity and quality of forests, and their protection are integral parts of current global and regional policies [38]. These factors, along with the increasing prices of wood and logistic challenges, have forced the particleboard industry to find alternative raw materials.

Many alternative raw materials, including kenaf, flax, hemp, miscanthus, vine pruning, canola stalks, sorghum, rice stalks, and wheat stalks, have previously been employed for manufacturing particleboards [24,29,42,52,56]. Some lignocellulosic materials can be cultivated for this purpose, such as kenaf and miscanthus; others are derived as residues during crop harvesting, for example, canola and wheat stalks. Although 5.9 million tons of stalk residues alone were produced worldwide in 2018 [20,59], their availability is strongly affected by seasonal cultivation and local conditions. In addition, the influence of prolonged storage on the properties of many such materials is largely unknown. However, only a few alternative lignocellulosic materials have successfully been used at an industrial scale. This is attributed to their lower mechanical strength, a high proportion of fine particles, and high mineral content. Increased adhesive content and adjusted press factors could compensate for some of the disadvantages in order to obtain performant particleboards, which in turn negatively affects the

* Corresponding author.
*E-mail address:* stergios.adamopoulos@slu.se (S. Adamopoulos).

https://doi.org/10.1016/j.mtcomm.2023.106602
Received 30 March 2023; Received in revised form 21 May 2023; Accepted 3 July 2023
Available online 5 July 2023

production costs. The majority of the tested materials were harvesting residues from agricultural operations. Process residues from the agricultural industry, such as sugar peep pulp, walnut husk, or olive stones, have been studied less [15,44].

The increased interest in finding agro-industry process residues has brought attention to barley husks, oat husks, and wheat bran. The benefits of these by-products are their continuous production over the year, the existing integration in logistical transport processes, and high-volume availability [40]. Barley and oat are common cereal grains. The husks, the protective surroundings, are lignocellulosic agro-waste fractions, which account for 20% of the harvested material. The barley and oat husks are mechanically separated from the grain in industrial processing. A small portion of husks is used as cattle food, fertiliser, or energy resource [13]. Wheat bran is currently an undervalued by-product of the cereal industry, which is produced in vast quantities worldwide [4]. Bran is the outer layer of the wheat grain itself, obtained during flour production, and it can be up to 25% of the grain weight [57]. Wheat bran is used as an animal feed or food additive as it has a high fibre content [51].

Different husks have been examined previously as raw materials for panel manufacturing [40]. In general, husks are suited for both fiberboard and particleboard but in order to meet the standard requirements for these products a combination with wooden material seems to be necessary. Silva et al. [63] used castor husks alone or in combination with pine wood chips and urea-formaldehyde (UF, 8 wt%) for particleboards. It was observed that the water resistance of the particleboards improved as the castor husks ratio increased. This improvement was explained by the particle geometry of husks, which enabled an increase of compression ratio and a less porous structure in the panels. Up to a proportion of 50% castor husks, internal bond strength and modulus of rupture remained constant, and even modulus of elasticity increased slightly. However, these mechanical propteries decreased with a share of 75% castor husks. The increasing proportion of rice husks in pine wood particleboards bonded by UF (12 wt%) increased their water absorption [64]. The rice husks could only achieve an insufficient bond quality, and the particle geometry created many voids that reduced the contact areas between the husk particles and the adhesive. Varanda et al. [53] manufactured single-layer particleboards with oat husks and polyurethane adhesive (10 wt%) and reported comparable thickness swelling and higher static bending strength than reference particleboards with eucalyptus wood. However, the interaction between the furnished material and the adhesive cannot be traced precisely since the properties of oat husks that are relevant for panels are largely unknown. This also applies to barley husks and wheat bran.

In order to evaluate the suitability of barley husks, oat husks, and wheat bran as the main furnish materials in particleboard manufacturing, their properties must be understood and compared with industrial wood chips. This study examined their chemical composition, acidity and buffering capacity, particle geometry, and mechanical strength. In order to elucidate their anatomical and microstructural characteristics, it was employed light microscopy, scanning electron microscopy, and X-ray microcomputed tomography.

## 2. Materials and methods

Barley husks (BH, *Hordeum vulgare*), oat husks (OH, *Avena sativa*), and wheat bran (WB, *Triticum aestivum*) were kindly provided by Lantmännen AB (Stockholm, Sweden). Industrial grade wood particles (WP) were supplied from the particleboard production line of IKEA Industry (Hultsfred, Sweden), divided as a core-layer and surface-layer particles with a combination of spruce (*Picea abies*), pine (*Pinus sylvestris*), poplar (*Populus tremula*), birch (*Betula pendula*) and alder (*Alnus incana*).

Ethanol (≥99.5%) and toluene (≥99%) were ordered from VWR (Stockholm, Sweden), and sodium chlorite (80%) and sulfuric acid (98%) from Sigma-Aldrich (Stockholm, Sweden). Sodium hydroxide (100%) and acetic acid (≥96%) were purchased from MERCK (Darmstadt, Germany), and cyanoacrylate glue from Loctite (Henkel, Düsseldorf, Germany).

The raw materials were sieved (mesh size 0.125 mm) to reduce the impact of dirt and unfamiliar particles and conditioned at 20 °C and 65% relative humidity for at least 14 days prior to characterisation. In case it was needed, the materials were milled with a laboratory mill (Polymix PX-MFC 90 D, Kinematica, Malters, Switzerland) with a sieve size of 1 mm.

### 2.1. Chemical characteristics

#### 2.1.1. Chemical composition

Chemical analyses of the agro-industry residue materials included cold- and hot-water extraction, 1% sodium hydroxide solubility (NaOH), ethanol-toluene extractive content, which was followed by holocellulose and α-cellulose, and ash content. The following methods were used:

- ASTM D1110-21 (cold- and hot-water extractives)
- TAPPI T212 om-02 (1%-NaOH)
- TAPPI T204 cm-97 (ethanol-toluene extractive content)
- EN 15403:2011 (ash content)
- Rowell [47] (holo- and α-cellulose)

Rowell's [47] method makes use of an acetic acid and sodium chlorite treatment for 24 h to determine the hemicelluloses content, followed by a sodium hydroxide immerse procedure to define the α-cellulose content. Three independent measurements were carried out for each chemical analysis, and the mean value was calculated. The lignin ratio was calculated as the difference between the original oven-dried sample, ethanol-toluene extractive content, holocellulose, and ash content.

Fourier Transform Infrared (FTIR) Spectrometer (Alpha FTIR spectrometer, Bruker, Karlsruhe, Germany) was used to analyse the chemical structure of BH and OH in comparison with WP. The FTIR analysis was conducted with a versatile high throughput ZnSe ATR crystal, in a wavelength from 4000 to 750 $cm^{-1}$ at room temperature, accumulating 64 scans with a resolution of 4 $cm^{-1}$. The samples were oven-dried, and a background spectrum was collected before to exclude the signals not associated with the sample.

#### 2.1.2. Acidity and buffering capacity

The acidity (pH) was calculated as the mean of three measurements determined according to a method described by Adamopoulos et al. [2]. A calibrated VWR pH Enomenal IS2100l (Stockholm, Sweden) was used to measure one gram of oven-dry material, soaked for 24 h at 20 °C in 20 ml distilled water. For the determination of the buffering capacity, the same solution was titrated with 0.05 N sodium hydroxide to a pH of 10 or with sulfuric acid to a pH of 3. After each increment (ml) of base or acid solution, the pH was noted when it reached a constant value for 2 min [43]. In addition to BH, OH, and WB, the acidity and buffering capacity of industrial WP were determined. The WP offer a comparative example of a currently used wood mix for particleboard production but only reflect a factory location-specific situation.

### 2.2. Structural and mechanical properties

#### 2.2.1. Bulk density and particle size

The bulk density was determined gravimetrically and calculated as the quotient of mass and volume (one litre). The result was reported as a mean of three measurements.

A digital particle size determination was carried out using the image analysis sensor QICPIC with the free-fall shaft GRADIS and VIBRI feeder (Sympatec, Clausthal-Zellerfeld, Germany). Approximately two grams of sample material was automatically fed from the hopper at a feed rate of 20%. The particle length was equated to the maximum Feret diameter

(Feret Max) and the particle width to the minimum Feret diameter (Feret Min). The Feret Max describes the longest distance between two parallel tangents on opposite sides of the projected particle, and the Feret Min accordingly as the shortest distance. Both parameters were set in relation to the volume ($Q_3$). Furthermore, the Feret Min is used as a comparable parameter to the sieve hole diameter in classic sieve analysis [25]. For particle size analysis, the core- (WP/CL) and surface-layer (WP/SL) fractions of the wood particles were examined separately as a comparative example.

#### 2.2.2. Anatomical structure

The anatomical structure was determined by the type of cell and its arrangement in relation to one another. The surfaces of the samples and their macrostructures were examined with a digital microscope (Keyence VHX-S550E, Osaka, Japan) equipped with a universal objective (VH-Z100UR).

Structural studies of the surfaces at higher magnifications were performed in the low-vacuum mode of an environmental scanning electron microscope (ESEM; FEI Quanta 600 FEG). Dry samples were mounted on aluminium stubs with carbon tape. The chamber pressure in the low vacuum mode was 0.75 Torr, and the acceleration voltage was 5 keV.

In order to examine the internal structure of the samples in a non-destructive way, x-ray micro-computed tomography (microCT) scans were carried out with a RXsolutions EasyTom 160. Scanning parameters of the nanofocus tube (diamond target and LaB6 filament) were set to 78 μA current and 70 kV tube voltage. The exposure time of the flat panel detector was 0.5 s, the number of average frames was 8, and the voxel size was 2.09 μm.

#### 2.2.3. Microfibril angle measurements

The microfibril angle (MFA) is defined as the orientation of the cellulose microfibrils in the secondary cell wall with respect to the long axis of cells. It is known as one of the main influencing factors on the mechanical properties of lignocellulosic materials [19].

The MFA was determined using wide-angle x-ray scattering (WAXS) on a Bruker AXS Nanostar equipped with a 2D Vantec 2000 area detector (Bruker Karlsruhe, Germany). Individual samples fixed vertically on a specimen holder were exposed to x-ray radiation with a wavelength of 1.54 Angstrom (Cu Kα) and a detector distance of 5.1 mm. Diffraction images were taken with a 30-min exposure time. The recorded 2D diffraction patterns were integrated, and the cellulose MFA was evaluated by the azimuthally scattering intensity distribution of the cellulose 002 reflection according to the method described by Lichtenegger [36]. The final MFA values were based on three particles per sample type and four measurement points for each particle. Since WP/SL and WP/CL originate from the same raw material, only WP/SL particles were examined.

#### 2.2.4. Microtensile test

The mechanical properties were determined with a custom-built microtensile testing device [17]. The materials tested were: inner oat husks (OHI), BH, WB, and WP. Since the vascular bundles are clearly visible in the outer OH and the microtensile test samples only have small dimensions, outer OH with vascular bundles (OH+VB) and outer OH without vascular bundles (OH-VB) were tested in order to be able to assess the influence on the mechanical strength. Longitudinal sections ($n = 10$), with a length of approximately 8 mm (OH, WP), 6 mm (BH), and 4 mm (WB), and a width of 0.3 – 0.6 mm, were prepared with a razor blade under a light microscope. Particles from WP/SL were used as a reference because they already had comparable sizes. The samples were glued onto polyester frames with cyanoacrylate glue under a light microscope. Tensile tests were performed after 24 h.

The samples were fixed to the microtensile testing device using pinholes, and the existing polyester support structures were then melted. Sample length and strain were determined by video extensometry. The tensile tests were carried out at approximately 26 °C and 30% relative humidity at a test speed of 5 μm/s with a 50 N maximum capacity load cell.

For the calculation of the ultimate stress and modulus of elasticity, the cross-sectional areas of the samples were determined. The samples were cut close to the fracture surface with a razor blade and observed under a scanning electron microscope (ESEM; FEI Quanta 600 FEG) in low-vacuum mode [16]. The total area was calculated using ImageJ software.

### 2.3. Statistical analysis

One-way analysis of variance (ANOVA) was performed with Origin Lab software (2021b SR2, Northampton, USA). The statistical differences between the values were evaluated by Tukey's honestly significant difference at an error probability of $\alpha = 0.05$.

## 3. Results and discussion

### 3.1. Chemical composition, acidity, and buffering capacity

The chemical characteristics of barley husks (BH), oat husks (OH), wheat bran (WB), softwood (SW, spruce), hardwood (HW, poplar), and industrial wood particles (WP) are shown in Table 1.

The holocellulose content of BH (70.81%) and OH (66.19%) are similar to the SW literature value. With 48.50%, WB had a noticeably lower holocellulose content. The proportion of α-cellulose in BH, OH, and WB were 28.32%, 29.80%, and 18.60%, and their lignin contents were 20.02%, 25.44%, and 43.57%, respectively. The values differed statistically (Table 1). With 5.35%, 6.27%, and 6.76%, BH, OH, and WB had approximately twenty times higher ash content compared to SW (0.3%) and HW (0.4%), which was also reported by Abedi and Dalai [1].

The extractive content of the materials was evaluated by cold- and hot-water, 1%-NaOH, and ethanol-toluene. WB had the highest cold-water extraction content of 23.73%, followed by oat OH with 13.94%. The difference in the cold-water solubility of BH (8.35%) and WP (6.81%) was statistically insignificant. The hot-water extraction portion for the three samples BH (10.67%), OH (16.98%), and WB (26.67%) were, in each case, 2–3% higher than the respective cold-water extraction value. The 1%-NaOH solubility of BH, OH, and WB were 47.28%, 42.08%, and 63.34%, respectively, and significantly higher than SW (12.0%) and HW (18.0%). WB has the lowest ethanol-toluene extraction content of 1.71%, OH of 2.10%, and BH of 3.82%, and are in the range of values reported for SW and HW by Rowell [47].

The influence of the chemical composition of the raw material on particleboard properties has already been well described. Cellulose and lignin are the skeleton of lignocellulosic materials and give them strength and internal cohesion. In general, it can be said that high cellulose content is related to high mechanical strength [7]. Extractives and lignin are more hydrophobic substances and can reduce water absorption in particleboards. Extractives, in particular, can have different effects, such as disrupting the bonding behaviour of the adhesives or reducing the amount of formaldehyde emissions [46]. Ash has a negative impact on particleboard properties. Since ash presents no wettability, adhesive distribution and adhesion are reduced [8]. Schmitz and colleagues reported potassium and calcium as the main minerals in the ash of OH [49]. BH and OH might be viable alternatives to wood in terms of their cellulose-to-lignin ratio. BH and OH generally differ only slightly in their composition. However, the high extractive and ash content compared to wood must be taken into account.

BH, OH, and WB are annual growing materials. Therefore, the annual weather conditions also have a major impact on the chemical composition of the raw materials. A comparison of the chemical composition of OH from two different seasons, made by Schmitz et al. [49], showed a significant variance. In a very warm and dry year (2018), the lignin content decreased from 24.4% (2016) to 12.9% and the cellulose

**Table 1**
Chemical composition (%), acidity, and buffering capacity (ml/ml) of barley husks, oat husk, wheat bran, softwood (spruce), hardwood (poplar), and industrial wood particles.

| | Barley husks (BH) | Oat husks (OH) | Wheat bran (WB) | Softwood (SW) | Hardwood (HW) | Wood particles (WP) |
|---|---|---|---|---|---|---|
| Holocellulose | 70.81 ± 0.82[a] | 66.19 ± 0.58[b] | 48.50 ± 0.11[c] | 69.0 * | 78.0 * | - |
| α-Cellulose | 28.32 ± 0.29[b] | 29.80 ± 0.11[a] | 18.60 ± 1.06[c] | 43.0 * | 49.0 * | - |
| Lignin | 20.02 ± 0.40[c] | 25.44 ± 0.41[b] | 43.57 ± 0.92[a] | 29.0 * | 19.0 * | - |
| Ash | 5.35 ± 0.06[c] | 6.27 ± 0.08[b] | 6.79 ± 0.02[a] | 0.3 * | 0.4 * | - |
| Extractives | | | | | | |
| Cold-water | 8.35 + 2.71[c] | 13.94 ± 0.28[b] | 23.73 ± 0.50[a] | 2.4 * | 5.0 * * | - |
| Hot-water | 10.67 ± 2.02[c] | 16.98 ± 1.26[b] | 26.67 ± 0.92[a] | 3.0 * | 6.0 * * | - |
| 1%-NaOH | 47.28 ± 1.78[b] | 42.08 ± 1.13[c] | 63.34 ± 2.44[a] | 12.0 * | 18.0 * | - |
| Ethanol-Toluene | 3.82 ± 0.53[a] | 2.10 ± 0.39[b] | 1.71 ± 0.45[c] | 2.0 * | 3.0 * | - |
| Buffering capacity | | | | | | |
| Acid equivalent | 0.0071 | 0.0046 | 0.0149 | - | - | 0.0049 |
| Alkaline equivalent | 0.0168 | 0.0138 | 0.0373 | - | - | 0.0059 |
| Total | 0.0239 | 0.0184 | 0.0522 | - | - | 0.0108 |

Mean ± SD Values followed by different superscripts (a,b,c,d) in the same row are significantly different ($p \leq 0.05$), * data obtained from [47], * * data obtained from Devappa et al. [18]

content from 33.1% to 24% in OH. In extreme weather conditions, OH invests more energy in building up proteins and lipids than lignocellulose. The fluctuating raw material properties are a challenge for particleboard production because these parameters can have a considerable influence, as described previously.

Other components, such as proteins and starch, can be present in BH, OH, and WB in higher concentrations compared to wood and can affect particleboard properties [41]. Proteins can act as a bio-based adhesive, thereby improving mechanical properties and increasing water resistance. Soy protein adhesive in wood-based panels, for example, has been extensively studied with promising results [6]. The current development of starch-based adhesives also reflects the positive influence in wood-based panels [37,39].

The chemical structure of the BH, OH, WB and WP were studied by FTIR spectroscopy (Fig. 1).

All samples showed a broad absorption band at 3200–3500 $cm^{-1}$ that is attributed to the stretching of hydroxyl groups in cellulose, hemicelluloses and lignin [61]. BH, OH and WB illustrated vibrations at 2930 and 2850 $cm^{-1}$, which might be related to the C–H bond stretching in cellulose and hemicelluloses [58]. The peak at 2930 $cm^{-1}$ is more intense than at 2850 $cm^{-1}$, whereas WP shows a more narrow band in the intermediate range. Rajkumar and Somasundaram [62] observed similar absorption bands in wheat husks and related them to asymmetric alkyl groups' stretch C–H bonding. The peaks at 1738 $cm^{-1}$ and 1642 $cm^{-1}$ could be related to the C═C linkage in the aromatic ring of lignin. Aryl-alkyl ether bonds (C-O-C) are present in cellulose and lignin and are indicated by a peak at 1260 $cm^{-1}$ [60]. WP had a greater absorption here because cellulose and lignin together make up 68–72% of the chemical composition, while it is 48% for BH, 62% for OH, and 62 for WB (Table 1). The adsorption band at 1022 and 1149 $cm^{-1}$ was due to C-O stretching vibration. The FTIR spectra of the studied alternative materials and WP are comparable as they are largely consistent of the three main components cellulose, hemicelluloses, and lignin.

The results of the acidity measurements are given in Table 1. BH and WB, with 6.84 and 6.81, had similar pH values and were close to the neutral region. The OH pH value was slightly lower at 6.36. WP had a more acid character with a significantly lower acidity value of 4.82.

Fig. 2 and Table 1 present the acid and base buffering capacities of BH, OH, WB, and WP. The acid equivalent of BH, OH, and WP differed only slightly, with a range of 0.0046–0.0071 ml/ml. On the one hand, WB had approximately three times higher acid buffering capacity of 0.0149 ml/ml. On the other hand, the base buffering capacity differences were greater between the samples. WP had the lowest alkaline equivalent (0.0059 ml/ml), followed by OH (0.0138 ml/ml) and BH (0.0168 ml/ml). WB had again a significantly higher buffering capacity (alkaline) of 0.0373 ml/ml.

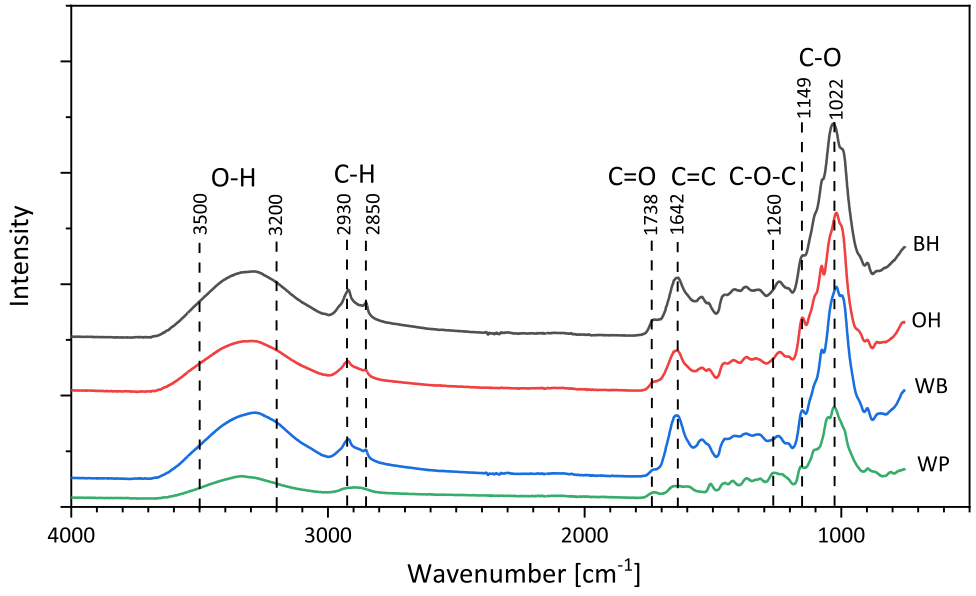


**Fig. 1.** FTIR analysis of barley husks (BH), oat husks (OH), wheat bran (WB), and industrial wood particles (WP).

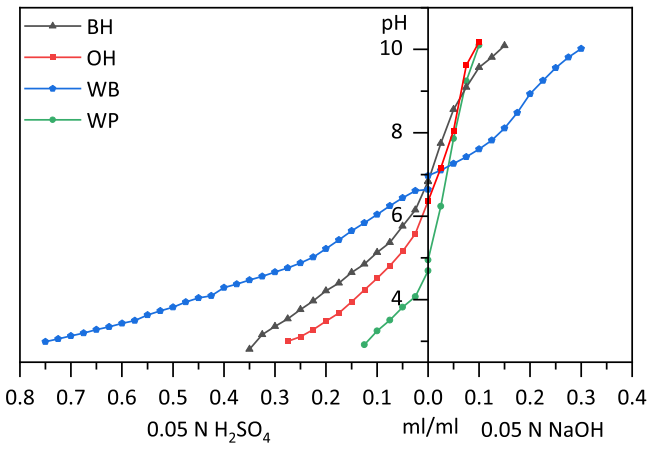


**Fig. 2.** Buffering capacity of barley husks (BH), oat husks (OH), wheat bran (WB), and industrial wood particles (WP).

The pH and buffering capacity are relevant factors for the interaction between the furnish materials and the adhesive in particleboards. For example, acidity influences the curing and binding behaviour of the adhesive system. Both values, pH and buffering capacity of the lignocellulosic materials depend on their chemical composition and the concentration and types of extractives [14]. Extremely low or high pH values at the wood-adhesive interface negatively affect the bondline [31] and can lead to lower mechanical strength. For example, a strongly acidic material reduces the gel time of urea-formaldehyde adhesives. Furthermore, high acidity can lead to the corrosion of fasteners in wood constructions [55].

Due to the fairly neutral acidity of BH, OH, and WB, no extreme pH values are to be expected. Of the samples analysed here, OH seems to be most suitable for particleboards in terms of acidity. However, most adhesive systems require a precise pH range (acid- or alkaline-catalysed) to cure appropriately. The high buffering capacity of WB makes it challenging to set the desired pH range correctly [3]. In order to make a definite statement about the influence of WB's high total buffering capacity on an adhesive system, their extractives should be examined in more detail.

### 3.2. Bulk density and particle size distribution

The size of wood particles is an essential controllable factor in particleboard manufacturing. Previous studies showed that the particle geometry, and in particular the ratio of length to width (aspect ratio), greatly influences the panel properties [11]. Long, narrow shapes with a correspondingly high aspect ratio lead to significantly higher mechanical strength than cubic particles with a low aspect ratio since they allow more contact surface between the particles [28]. Two different size classes are generally used for the production of industrial panels like particleboards. Particles for the surface layers (SL) are significantly smaller than particles for the core layer (CL). Smaller particles (WP/SL) are used at the surface to achieve an even structure and a low-pored layer for coatings. The larger wood particles for the middle part of the panel (WP/CL) primarily improve the bending properties due to their dimensions [26]. Since the particle sizes differ depending on the product and production parameters, the samples WP/SL and WP/CL analysed in this study can only serve as indicative examples. Fig. 3 shows the results of image analysis measurements.

WP/SL had an average particle length of 2.92 mm and a width of 0.85 mm. In contrast, WP/CL had an average length of 4.87 mm and a width of 1.7 mm. WP/SL corresponded to a classic Gaussian normal distribution regarding size distribution. However, the particle size distribution of WP/CL was quite broad, thus showing a higher variation. The mean particle length of BH was 3.92 mm, less than half of that of OH (8.33 mm). The width of the BH and OH particles was 1.24 mm and 1.87 mm, respectively. Both samples showed a very sharp and narrow size distribution. The particle size distribution of WB was noticeably broader, with an average length of 2.31 mm and a width of 0.59 mm.

BH and OH were not subjected to any pre-treatment other than mechanical removal from the grain. The narrow particle size distribution corresponded to their natural husk shape. Therefore, the two materials have a very homogeneous particle geometry, which is a reasonable basis for further processing. Although slightly broader, the particle size distribution of WB was comparable to that of WP/SL. OH particles clearly had the highest aspect ratio (4.47), followed by WB (3.92) and WP/SL (3.44). BH had an aspect ratio of 3.16, and WP/CL had the lowest aspect ratio of 2.86. The calculated low aspect ratio of WP/CL can result from the broad particle size distribution. BH seems to have particle geometries between surface and core layer WP and could serve as a connection layer between the coarse core and fine surface material in a multi-layer panel. The large particle size of OH could be used in the core zone of classic particleboards, and their high aspect ratio would promote bending properties.

Feret Max and Min were determined by image analysis using the projected particles. Since an image of the particles in free fall is recorded with the QICPIC instrument, the complete maximum area is rarely projected. Consequently, the ferret diameters tend to underestimate the actual size somewhat. At the same time, measuring the particle thickness directly is impossible. Nevertheless, particle thickness seems to have little effect on particleboard properties [12]. The long particles of OH or a combination of BH and OH could be suitable for the core layer in particleboards.

The bulk density of BH was the lowest, 152 $kg.m^{-3}$, as compared with OH (163 $kg.m^{-3}$) and WB (167 $kg.m^{-3}$). They are thus between the bulk density values of WP/SL (183 $kg.m^{-3}$) and WP/CL (141 $kg.m^{-3}$) (Fig. 4). Due to the similar weight per volume unit, processing of all the agro-industry materials should be possible with the same machine types used for wood particles.

### 3.3. Anatomical structure

The anatomical structure of the husk samples (BH, OH) and WB were examined using digital microscopy, microCT, and ESEM. The exemplary illustrations correspond to the appearance of the majority of the samples.

#### 3.3.1. Barley husks

Fig. 5 shows the anatomy of the BH material. The optical micrographs illustrate a difference between the natural husk form and the industrial by-product (Fig. 5A). Natural BH has the awn attached. In the industrial material, the awns have been removed. Most awns already break off during harvesting in the combine harvester since they cannot withstand mechanical stress. MicroCT scans of the cross-section (Fig. 5B) confirmed that the husk material is leaf structured. The intermediate layer, consisting of bast fibres and spongy parenchyma, is surrounded by the inner and outer epidermis. On the outer epidermis, it exists a thin layer of wax, the cuticle [10]. Another leaf-typical feature is the vascular bundles, which can be seen on the outside and inside of the BH. The outer surface has a dotted structure (Fig. 5C), the trichome basis. The trichomes might inhibit bonding between particles in the panel. Kurokochi and Sato [33] reported that the contact area between the particles decreases due to the trichome base of rice straw, thus affecting the mechanical properties. The trichomes were broken through fine grinding of the rice straw particles, and the mechanical properties and water resistance of binderless particleboards were improved [32]. Furthermore, the trichomes of wheat husks showed a high concentration of silicon, which could affect the adhesive bond [27].

#### 3.3.2. Oat husks

The representations and results of the different examination methods

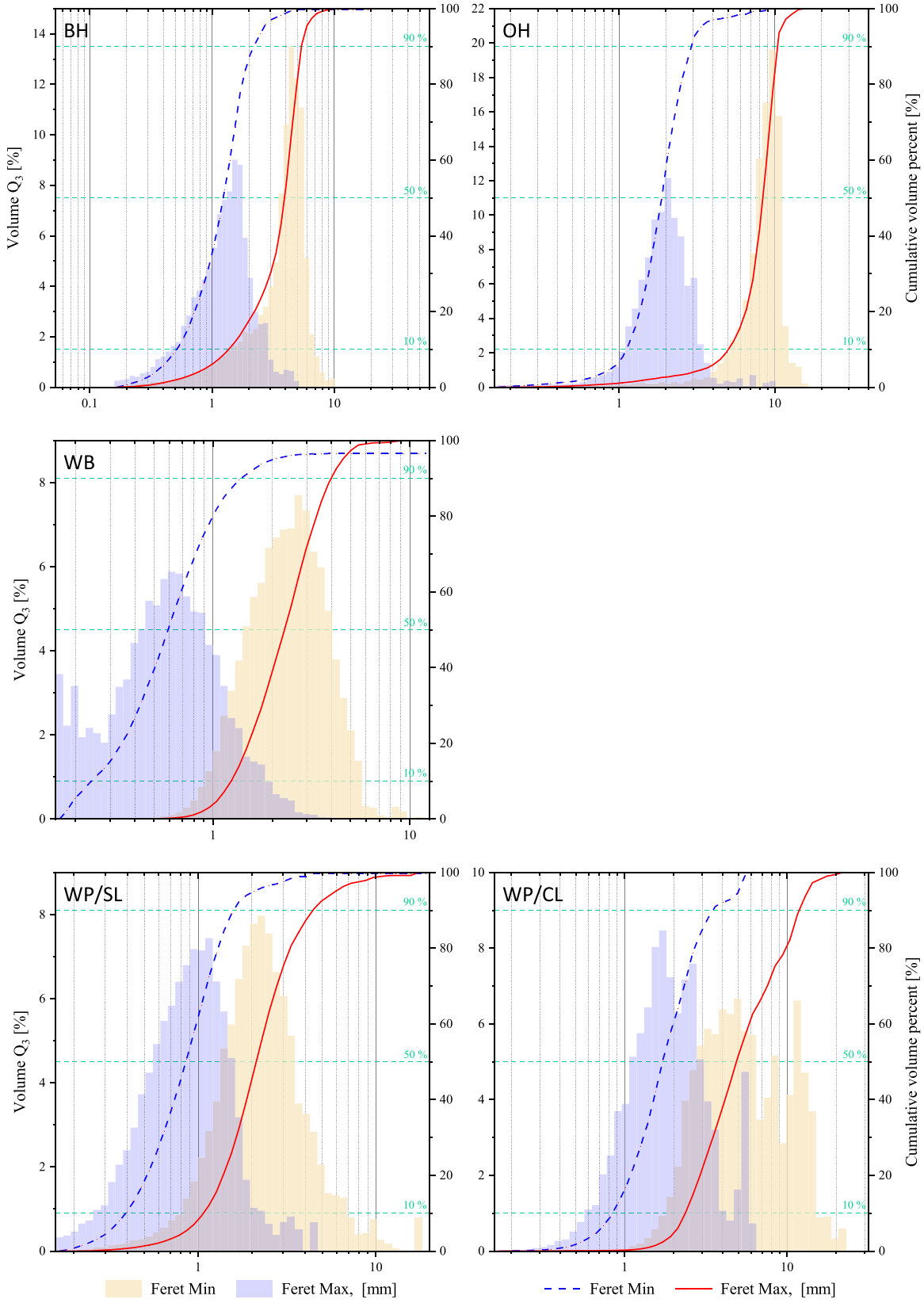


**Fig. 3.** Particle size distribution of barley husks (BH), oat husks (OH), wheat bran (WB), surface layer wood particles (WP/SL), and core layer wood particles (WP/CL). Feret Min distribution (blue bars and slope), Feret Max distribution (orange bars and red slope).

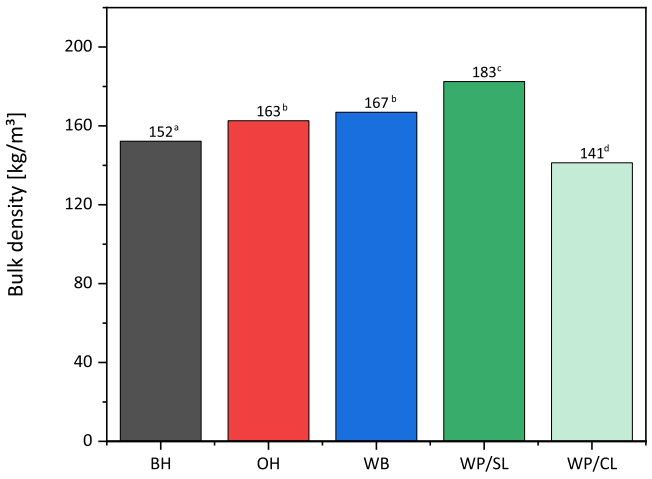


**Fig. 4.** Bulk density of barley husks (BH), oat husks (OH), wheat bran (WB), surface layer wood particles (WP/SL), and core layer wood particles (WP/CL); values followed by different superscripts (a,b,c,d) are significantly different ($p \leq 0.05$).

of OH are shown in Fig. 6. Compared to BH, OH are significantly larger and do not have an awn. The husks consist of larger outer parts (lemma), and the smaller and narrower inner part (palea), which can also be seen inside shots as shown in Fig. 6A [34]. The vascular bundles are also clearly visible. Investigation on the oil palm trunk describes the vascular bundles as less hygroscopic than the surrounding parenchymal tissue [45]. Therefore, the pronounced vascular bundles in OH could also help to reduce the water absorption in a particleboard panel. For the mechanical characterisation of OH, the vascular bundles were taken into account when preparing the samples. In contrast to BH, OH were less damaged and resembled their natural shape. In addition, they largely retained their cylindrical shape when enclosing the grain. This is a clear difference compared to the other materials of the present study. A leaf structure could be seen (Fig. 6B) as well as the trichome bases on the outside of the OH (Fig. 6C).

### 3.3.3. *Wheat bran*

WB is the screened material when wheat flour is produced and can be considered a by-product. Bran, in general, is the outer thin layer of the grain. It consists of the pericarp, seed coat, and the first cell rows of aleurone and sub-aleurone [23]. In the aleurone region, the material is separated from the main component of the grain, the endosperm. White areas can be seen on the inside of the wheat bran (Fig. 7A), which can be associated with the endosperm and its components, like starch, oils, or proteins [48]. The chemical composition analysis (Table 1) showed high content of cold- and hot-water, and 1%-NaOH extractives. Even if the endosperm components were not directly soluble in water, they could have been separated from the aleurone layer and filtered out during the

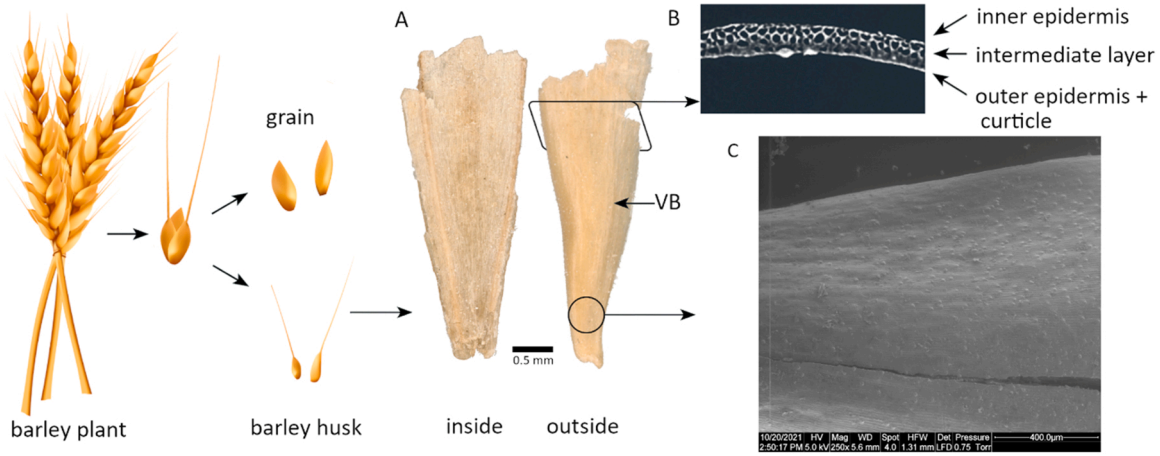


**Fig. 5.** Origin and anatomy of barley husk (BH). Images were taken with digital microscopy (A), microCT (B) and ESEM (C), Vascular bundle (VB).

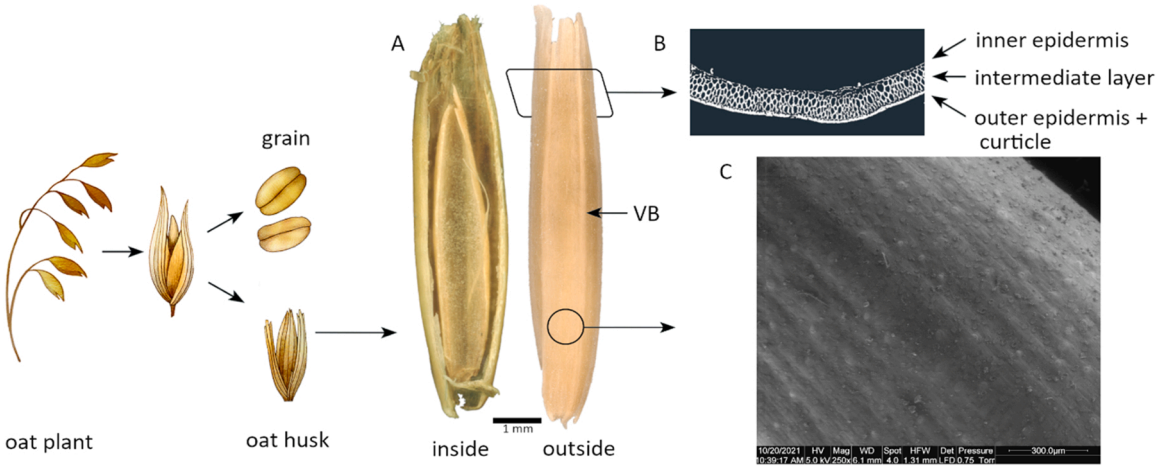


**Fig. 6.** Origin and anatomy of OH. Images were taken with digital microscopy (A), microCT (B) and ESEM (C), Vascular bundle (VB). Partly adopted from Grundy et al. [23].

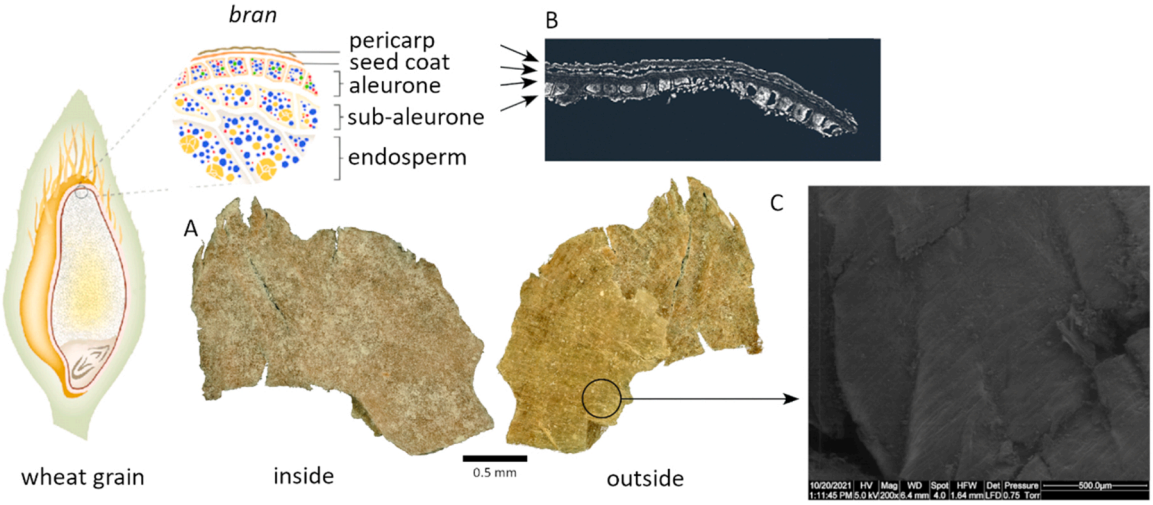


**Fig. 7.** Origin and anatomy of WB. Images were taken with digital microscopy (A), microCT (B), and ESEM (C). Partly adopted from Grundy et al. [23].

measurement. The microCT image (Fig. 7B) also shows that the pericarp and, in part, the seed coat have been separated from the other cell layers. The poor bonding between these layers was noted in all investigations. The results of the strong mechanical stresses that were applied to the material during flour production could be seen in the digital microscope (Fig. 7A) and the ESEM images (Fig. 7C), as the material was severely damaged and compressed.

Due to harvesting or processing by a machine, BH have been reduced in size more than OH. Both materials have a homogeneous cell structure except for the vascular bundles. The trichome bases could be identified on both husks' outsides, with BH having more trichome bases but smaller ones compared to OH. The outer wax layer, the cuticle, should be examined more closely in future studies in order to be able to estimate its effect on particleboards. Studies on wax extraction with hexane on rice straw report improved self-bonding properties in particleboards [32]. Different husk types, such as inner and outer OH, could not be noted with the BH and WB material. The anatomical structure of WB is, however, considerably different from the two other husk materials. The outer layer of the wheat grain was severely deformed during processing, and the individual layers have little adhesion to one another, which may limit its performance under load-bearing.

### 3.4. MFA and microtensile test

The microfibril angle (MFA) is formed between the cellulose microfibrils and the fibre's longitudinal axis and was determined by wide-angle x-ray scattering. The results of the MFA investigations are given in Fig. 8. OH has the highest value of 44.32°. The BH and the inner OH (OHI) have similar MFA with 36.84° and 37.35°, respectively. WP/SL had the lowest MFA of 11.14°.

The relation between MFA and compressive strength, as well as shrinkage behaviour, was shown in previous studies [22,50]. Comparative values of the MFA from the literature are given in a range of 9°– 28.6° for different pine types [30], eucalyptus with 0°– 13° [54], and 7.8–28° for poplar [50]. Therefore, WP/SL's MFA is in accordance with previous studies. However, the MFA of BH and OH is significantly higher than typical wooden materials. A high MFA usually decreases the mechanical strength of the lignocellulosic material and increases the longitudinal shrinkage component [9].

A successful determination of the MFA of WB could not be carried out. The failure might be due to the multi-layer structure of the material. Antoine et al. [5] investigated the mechanical properties of the individual WB layers (pericarp, intermediate layer, and aleurone layer). Their results showed significant differences between the pericarp and

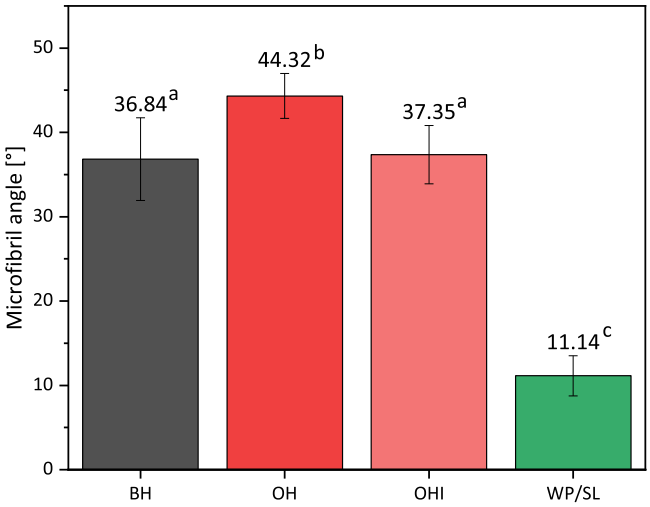


**Fig. 8.** Microfibril angle of barley husks (BH), oat husks (OH), inner oat husks (OHI), and surface layer wood particles (WP/SL). Values followed by different superscripts (a, b, c) are significantly different ($p \leq 0.05$).

the other two layers and recommended the separation of these layers in the case of mechanical application. The variation is attributed to the strongly heterogeneous cell wall components between the layers. Another reason could be different MFAs in each layer, which is why no clear MFA could be determined in this study. Likewise, no MFA value could be found in the literature. For a successful MFA determination of WB, individual parameters in the WAXS measurement should be adjusted, or separate measurements for each WB layer should be carried out.

The tensile properties of BH, OH without (OH-V) and with (OH+V) vascular bundle, OHI, WB, and WP/SL are presented in Fig. 9.

BH had an ultimate stress of 120.69 MPa and a modulus of elasticity (MOE) of 2.77 GPa. The different OH ultimate stress values were 169.48 (OH-V), 143.71 (OH+V), and 156.38 MPa (OHI) and did not differ statistically significantly. Their MOE values were 1.14, 0.84, and 2.42 GPa, respectively. WB's ultimate stress was 49.16 MPa, while the MOE was 1.45 GPa. An ultimate stress of 172.52 MPa and a MOE of 4.39 GPa was found for WP/SL.

The similar MFA of BH and OHI was reflected in the ultimate stress and MOE values that were not statistically different from each other. The

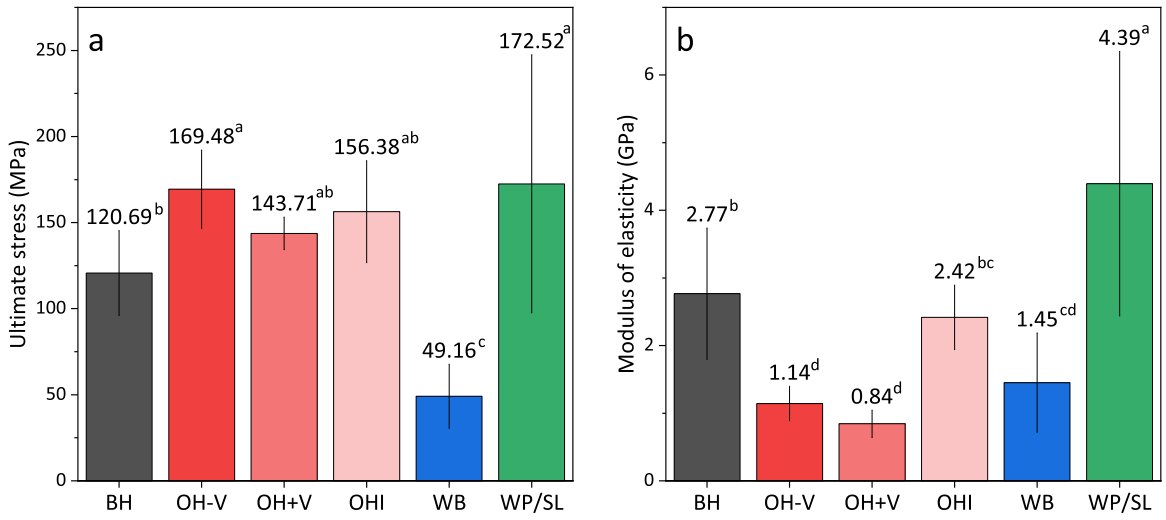


**Fig. 9.** Ultimate stress (a) and modulus of elasticity (MOE) (b) results from microtensile testing of burley husks (BH), oat husks without vascular bundle (OH-V), oat husks with vascular bundle (OH+V), inner oat husks (OHI), wheat bran (WB), and industrial wood particles (WP/SL). Values followed by different superscripts (a, b, c, d) are significantly different ($p \leq 0.05$).

outer OH (OH-V, OH+V), on the other hand, had a significantly lower MOE, although their ultimate stress was comparable to OHI. The lower MOE of OH-V and OH+V can be explained by the larger MFA. Li et al. [35] demonstrated with mechanical strength analysis on Chinese fir (*Cunninghamia lanceolata*) fibres that an increased MFA leads to reduced MOE. Furthermore, the results showed that although the vascular bundles were visible to the naked eye in the outer OH samples, they had no obvious impact on mechanical strength. Samples containing a vascular bundle had only slightly lower tensile strength. That might be due to small differences in the available cell wall mass that could provide stability. The increased separation of the WB layers, the low cellulose content (Table 1), and the unsuccessful determination of the MFA was already an indication of the low mechanical load-bearing capacity (Fig. 9). The great microtensile strength performance of WP/SL is in accordance with the previous investigations of chemical composition and MFA. Compared to the other materials, WP/SL has a higher cellulose content and a significantly lower MFA, which can lead to increased tensile strength [21]. The high standard deviation in tensile strength and MOE of WP/SL can be related to the material composition optimised for industrial applications. The OH material, as a composition of outer and inner husks, seems to be able to resist similar ultimate stress-strain like industrial wood particles, while it has a lower MOE and a more flexible character.

## 4. Conclusions

In this study, the chemical composition, anatomical structure, particle geometry, and mechanical properties of BH, OH, and WB were analysed with regard to their applicability in particleboard manufacturing. These agro-industry by-products have a comparable holocellulose content to wood but significantly higher extractive and ash content. The high microfibril angle of the OH samples was reflected in their lower mechanical strength. The multi-layer structure of WB is only a few cell layers thick, and they are hardly resilient.

The lower modulus of elasticity of the agricultural materials BH, OH and WB than WP might be limiting factor for their suitability as raw materials for particleboards in load-bearing applications. Still, BH could be used proportionately as a furnish material in particleboards for interior furniture since they showed the highest MOE and the lowest ash content compared to OH and WB. In addition, their particle size is between the surface and core layer wood materials. The cylindrical and concave structure of OH makes them attractive for uses in lightweight particleboards where thermal or acoustic insulation properties are desirable. WB could be used in particleboards as a filler material or acidity buffer to control the curing behaviour of adhesives. The high proportion of extractives in WB could be the basis for further investigations to increase their economic value.

Future investigations on the studied alternative materials should analyse their interaction with water or adhesives to asses technological limitations and production processes in particleboard manufacturing. Furnish mixtures, adhesive types and load levels, and process parameters should be explored to conclude whether the derived particleboards meet the minimum requirements of the European Norm (EN) 312: 2003 for respective particleboard types.

## Funding

This research was funded by Formas, grant number 2018–01371, project title: “Agro-industry feedstocks and side streams for increasing the sustainability of wood panel production”.

## CRediT authorship contribution statement

**Nicolas Neitzel**: Conceptualization, Methodology, Formal analysis, Investigation, Writing – original draft. **Michaela Eder**: Methodology, Investigation, Writing – review & editing. **Reza Hosseinpourpia**: Methodology, Writing – review & editing. **Thomas Walther:** Conceptualization, Methodology, Writing – review & editing. **Stergios Adamopoulos**: Conceptualization, Resources, Writing – review & editing, Supervision, Project administration, Funding acquisition.

## Declaration of Competing Interest

The authors declare the following financial interests/personal relationships which may be considered as potential competing interests: Stergios Adamopoulos reports financial support was provided by Formas (Swedish Research Council for Sustainable Development)

## Data Availability

Data will be made available on request. No data was used for the research described in the article.

## References


[1] A. Abedi, A.K. Dalai, Study on the quality of oat hull fuel pellets using bio-additives, Biomass Bioenergy 106 (2017) 166–175, https://doi.org/10.1016/j.biombioe.2017.08.024.

[2] S. Adamopoulos, E. Voulgaridis, C. Passialis, Variation of certain chemical properties within the stemwood of black locust (Robinia pseudoacacia L.), Holz als roh-und Werkst. 63 (2005) 327–333.

[3] A.A. Alade, Z. Naghizadeh, C.B. Wessels, L. Tyhoda, A review of the effects of wood preservative impregnation on adhesive bonding and joint performance, J. Adhes. Sci. Technol. 36 (2021) 1593–1617, https://doi.org/10.1080/01694243.2021.1981651.

[4] N. Annamalai, N. Sivakumar, Production of polyhydroxybutyrate from wheat bran hydrolysate using Ralstonia eutropha through microbial fermentation, J. Biotechnol. 237 (2016) 13–17, https://doi.org/10.1016/j.jbiotec.2016.09.001.

[5] C. Antoine, S. Peyron, F. Mabille, C. Lapierre, B. Bouchet, J. Abecassis, X. Rouau, Individual contribution of grain outer layers and their cell wall structure to the mechanical properties of wheat bran, J. Agric. Food Chem. 51 (2003) 2026–2033, https://doi.org/10.1021/jf0261598.

[6] A. Bacigalupe, M.M. Escobar, Soy protein adhesives for particleboard production – a review, J. Polym. Environ. 29 (2021) 2033–2045, https://doi.org/10.1007/s10924-020-02036-8.

[7] M. Baharoğlu, G. Nemli, B. Sarı, T. Birtürk, S. Bardak, Effects of anatomical and chemical properties of wood on the quality of particleboard, Compos. Part B: Eng. 52 (2013) 282–285, https://doi.org/10.1016/j.compositesb.2013.04.009.

[8] S. Bardak, G. Nemli, S. Tiryaki, The influence of raw material growth region, anatomical structure and chemical composition of wood on the quality properties of particleboards, Maderas Cienc. Y. Tecnol. (2017), https://doi.org/10.4067/s0718-221×2017005000031.

[9] J.R. Barnett, V.A. Bonham, Cellulose microfibril angle in the cell wall of wood fibres, Biol. Rev. Camb. Philos. Soc. 79 (2004) 461–472, https://doi.org/10.1017/s1464793103006377.

[10] C. Barron, U. Holopainen-Mantila, S. Sahlstrom, A.K. Hotekjolen, V. Lullien-Pellerin, Assessment of biochemical markers identified in wheat for monitoring barley grain tissue, J. Cereal Sci. 74 (2017) 11–18, https://doi.org/10.1016/j.jcs.2017.01.004.

[11] J.T.L. Bazzetto, G. Bortoletto Junior, F.M.S. Brito, Effect of particle size on bamboo particle board properties, Floresta e Ambient. (2019) 26, https://doi.org/10.1590/2179-8087.012517.

[12] J.T. Benthien, J. Lüdtke, M. Ohlmeyer, Effect of increasing core layer particle thickness on lightweight particleboard properties, Eur. J. Wood Wood Prod. 77 (2019) 1029–1043, https://doi.org/10.1007/s00107-019-01452-5.

[13] A.K. Bledzki, A.A. Mamun, J. Volk, Barley husk and coconut shell reinforced polypropylene composites: the effect of fibre physical, chemical and surface properties, Compos. Sci. Technol. 70 (2010) 840–846, https://doi.org/10.1016/j.compscitech.2010.01.022.

[14] S. Bockel, I. Mayer, J. Konnerth, P. Niemz, C. Swaboda, M. Beyer, S. Harling, G. Weiland, N. Bieri, F. Pichelin, Influence of wood extractives on two-component polyurethane adhesive for structural hardwood bonding, J. Adhes. 94 (2018) 829–845, https://doi.org/10.1080/00218464.2017.1389279.

[15] P. Borysiuk, I. Jenczyk-Tolloczko, R. Auriga, M. Kordzikowski, Sugar beet pulp as raw material for particleboard production, Ind. Crops Prod. (2019) 141, https://doi.org/10.1016/j.indcrop.2019.111829.

[16] I. Burgert, M. Eder, K. Frühmann, J. Keckes, P. Fratzl, S. Stanzl-Tschegg, Properties of chemically and mechanically isolated fibres of spruce (Picea abies [L.] Karst.). Part 3: mechanical characterisation, Holzforschung 59 (2005) 354–357, https://doi.org/10.1515/HF.2005.058.

[17] I. Burgert, K. Frühmann, J. Keckes, P. Fratzl, S.E. Stanzl-Tschegg, Microtensile testing of wood fibers combined with video extensometry for efficient strain detection, Holzforschung 57 (2003) 661–664, https://doi.org/10.1515/HF.2003.099.

[18] R.K. Devappa, S.K. Rakshit, R.F. Dekker, Forest biorefinery: Potential of poplar phytochemicals as value-added co-products, Biotechnol. Adv. 33 (2015) 681–716, https://doi.org/10.1016/j.biotechadv.2015.02.012.

[19] J. Erasmus, A. Kunneke, D.M. Drew, C.B. Wessels, The effect of planting spacing on Pinus patula stem straightness, microfibril angle and wood density, For. Int. J. For. Res. 91 (2018) 247–258, https://doi.org/10.1093/forestry/cpy005.

[20] Fao. 2022a. Food and Agriculture Organization - Database [Online]. Available: http://www.fao.org/faostat/ [Accessed 02. June 2022].

[21] M. Genet, A. Stokes, F. Salin, S.B. Mickovski, T. Fourcaud, J.-F. Dumail, R. Van Beek, The influence of cellulose content on tensile strength in tree roots, Plant Soil 278 (2005) 1–9, https://doi.org/10.1007/s11104-005-8768-6.

[22] P.R. Gherardi Hein, J. Tarcísio Lima, Relationships between microfibril angle, modulus of elasticity and compressive strength in Eucalyptus wood, Maderas Cienc. Y. Tecnol. (2012), https://doi.org/10.4067/s0718-221×2012005000002.

[23] M.M. Grundy, A. Fardet, S.M. Tosh, G.T. Rich, P.J. Wilde, Processing of oat: the impact on oat's cholesterol lowering effect, Food Funct. 9 (2018) 1328–1343, https://doi.org/10.1039/c7fo02006f.

[24] S. Halvarsson, H. Edlund, M. Norgren, Manufacture of high-performance rice-straw fiberboards, Ind. Eng. Chem. Res. 49 (2010) 1428–1435, https://doi.org/10.1021/ie901272q.

[25] P. Hamilton, D. Littlejohn, A. Nordon, J. Sefcik, P. Slavin, Validity of particle size analysis techniques for measurement of the attrition that occurs during vacuum agitated powder drying of needle-shaped particles, Analyst 137 (2012) 118–125, https://doi.org/10.1039/c1an15836h.

[26] R. Hashim, N. Saari, O. Sulaiman, T. Sugimoto, S. Hiziroglu, M. Sato, R. Tanaka, Effect of particle geometry on the properties of binderless particleboard manufactured from oil palm trunk, Mater. Des. 31 (2010) 4251–4257, https://doi.org/10.1016/j.matdes.2010.04.012.

[27] Š. Hýsek, M. Podlena, H. Bartsch, C. Wenderdel, M. Böhm, Effect of wheat husk surface pre-treatment on the properties of husk-based composite materials, Ind. Crops Prod. 125 (2018) 105–113, https://doi.org/10.1016/j.indcrop.2018.08.035.

[28] A.H. Juliana, M.T. Paridah, S. Rahim, I.N. Azowa, U.M.K. Anwar, Properties of particleboard made from kenaf (Hibiscus cannabinus L.) as function of particle geometry, Mater. Des. 34 (2012) 406–411, https://doi.org/10.1016/j.matdes.2011.08.019.

[29] A. Khazaeian, A. Ashori, M.Y. Dizaj, Suitability of sorghum stalk fibers for production of particleboard, Carbohydr. Polym. 120 (2015) 15–21, https://doi.org/10.1016/j.carbpol.2014.12.001.

[30] J.-Y. Kim, S.-C. Kim, B.-R. Kim, Microfibril angle characteristics of korean pine trees from depending on provinces, J. Korean Wood Sci. Technol. 48 (2020) 569–576, https://doi.org/10.5658/wood.2020.48.4.569.

[31] P. Król, R. Toczyłowska-Mamińska, M. Mamiński, A critical role for the presence of lignocellulosic material in the determination of wood buffering capacity, J. Wood Chem. Technol. 37 (2017) 478–484, https://doi.org/10.1080/02773813.2017.1347683.

[32] Y. Kurokochi, M. Sato, Effect of surface structure, wax and silica on the properties of binderless board made from rice straw, Ind. Crops Prod. 77 (2015) 949–953, https://doi.org/10.1016/j.indcrop.2015.10.007.

[33] Y. Kurokochi, M. Sato, Properties of binderless board made from rice straw: the morphological effect of particles, Ind. Crops Prod. 69 (2015) 55–59, https://doi.org/10.1016/j.indcrop.2015.01.044.

[34] X. Li, K. Zhang, B. Han, Y. Yang, Architecture of paleas and lemmas dominates seed shattering trait in naked oat (Avena nuda), Cereal Res. Commun. (2023), https://doi.org/10.1007/s42976-022-00347-1.

[35] Z. Li, T. Zhan, M. Eder, J. Jiang, J. Lyu, J. Cao, Comparative studies on wood structure and microtensile properties between compression and opposite wood fibers of Chinese fir plantation, J. Wood Sci. (2021) 67, https://doi.org/10.1186/s10086-021-01945-z.

[36] H. Lichtenegger, Determination of spiral angles of elementary fibrils in the wood cell wall: comparison of small-angle X-ray scattering and wide-angle X-ray diffraction, Micro Angle Wood (1998) 140–156.

[37] M.I. Maulana, M. a R. Lubis, F. Febrianto, L.S. Hua, A.H. Iswanto, P. Antov, L. Kristak, E. Mardawati, R.K. Sari, L.H. Zaini, W. Hidayat, V.L. Giudice, L. Todaro, Environmentally friendly starch-based adhesives for bonding high-performance wood composites: a review, Forests (2022) 13, https://doi.org/10.3390/f13101614.

[38] H. Moor, J. Eggers, H. Fabritius, N. Forsell, L. Henckel, U. Bradter, A. Mazziotta, J. Nordén, T. Snäll, Rebuilding green infrastructure in boreal production forest given future global wood demand, J. Appl. Ecol. 59 (2022) 1659–1669, https://doi.org/10.1111/1365-2664.14175.

[39] N. Neitzel, R. Hosseinpourpia, S. Adamopoulos, A dialdehyde starch-based adhesive for medium-density fiberboards, BioResources 18 (2023).

[40] N. Neitzel, R. Hosseinpourpia, T. Walther, S. Adamopoulos, Alternative materials from agro-industry for wood panel manufacturing-a review, Mater. (Basel) 15 (2022), https://doi.org/10.3390/ma15134542.

[41] O.O. Onipe, A.I.O. Jideani, D. Beswa, Composition and functionality of wheat bran and its application in some cereal food products, Int. J. Food Sci. Technol. 50 (2015) 2509–2518, https://doi.org/10.1111/ijfs.12935.

[42] A.N. Papadopoulos, J.R.B. Hague, The potential for using flax (Linum usitatissimum L.) shiv as a lignocellulosic raw material for particleboard, Ind. Crops Prod. 17 (2003) 143–147, https://doi.org/10.1016/s0926-6690(02)00094-8.

[43] C. Passialis, E. Voulgaridis, S. Adamopoulos, M. Matsouka, Extractives, acidity, buffering capacity, ash and inorganic elements of black locust wood and bark of different clones and origin, Holz als Roh-und Werkst. 66 (2008) 395–400.

[44] H. Pirayesh, A. Khazaeian, T. Tabarsa, The potential for using walnut (Juglans regia L.) shell as a raw material for wood-based particleboard manufacturing, Compos. Part B: Eng. 43 (2012) 3276–3280, https://doi.org/10.1016/j.compositesb.2012.02.016.

[45] S.F.M. Ramle, O. Sulaiman, R. Hashim, T. Arai, A. Kosugi, H. Abe, Y. Murata, Y. Mori, Characterisation of parenchyma and vascular bundle of oil palm trunk as function of storage time, Lignocellulose 1 (2012) 33–44.

[46] E. Roffael, Significance of wood extractives for wood bonding, Appl. Microbiol Biotechnol. 100 (2016) 1589–1596, https://doi.org/10.1007/s00253-015-7207-8.

[47] R.M. Rowell, Handbook of Wood Chemistry and Wood Composites, CRC Press, Boca Raton, FL, USA, Boca Raton, 2013.

[48] G.P. Savill, A. Michalski, S.J. Powers, Y. Wan, P. Tosi, P. Buchner, M. J. Hawkesford, Temperature and nitrogen supply interact to determine protein distribution gradients in the wheat grain endosperm, J. Exp. Bot. 69 (2018) 3117–3126, https://doi.org/10.1093/jxb/ery127.

[49] E. Schmitz, E. Nordberg Karlsson, P. Adlercreutz, Warming weather changes the chemical composition of oat hulls, Plant Biol. (Stuttg.) 22 (2020) 1086–1091, https://doi.org/10.1111/plb.13171.

[50] F. Sheng-Zuo, Y. Wen-Zhong, F. Xiang-Xiang, Variation of microfibril angle and its correlation to wood properties in poplars, J. For. Res. 15 (2004) 261–267, https://doi.org/10.1007/bf02844949.

[51] A. Sobota, Z. Rzedzicki, P. Zarzycki, E. Kuzawińska, Application of common wheat bran for the industrial production of high-fibre pasta, Int. J. Food Sci. Technol. 50 (2015) 111–119, https://doi.org/10.1111/ijfs.12641.

[52] F. Tröger, G. Wegener, C. Seemann, Miscanthus and flax as raw material for reinforced particleboards, Ind. Crops Prod. 8 (1998) 113–121, https://doi.org/10.1016/s0926-6690(97)10017-6.
[53] L.D. Varanda, M.F.D. Nascimento, A.L. Christoforo, D. a L. Silva, F. a R. Lahr, Oat hulls as addition to high density panels production, Mater. Res. 16 (2013) 1355–1361, https://doi.org/10.1590/s1516-14392013005000131.
[54] N.H. Vonk, M.G.D. Geers, J.P.M. Hoefnagels, Full-field hygro-expansion characterisation of single softwood and hardwood pulp fibers, Nord Pulp Pap. Res J. 36 (2021) 61–74, https://doi.org/10.1515/npprj-2020-0071.
[55] A. Wahyudianto, A. Fernandes, Erwin, Wajilan, Metal corrosion in wood joint products and structures: a review, Int. J. Corros. Scale Inhib. (2022) 11, https://doi.org/10.17675/2305-6894-2022-11-3-21.
[56] J. Xu, R. Widyorini, H. Yamauchi, S. Kawai, Development of binderless fiberboard from kenaf core, J. Wood Sci. 52 (2006) 236–243, https://doi.org/10.1007/s10086-005-0770-3.
[57] Y. Zhang, X. Song, Y. Xu, H. Shen, X. Kong, H. Xu, Utilisation of wheat bran for producing activated carbon with high specific surface area via NaOH activation using industrial furnace, J. Clean. Prod. 210 (2019) 366–375, https://doi.org/10.1016/j.jclepro.2018.11.041.
[58] S. Banerjee, G.C. Sharma, R.K. Gautam, M.C. Chattopadhyaya, S.N. Upadhyay, Y. C. Sharma, Removal of Malachite Green, a hazardous dye from aqueous solutions using Avena sativa (oat) hull as a potential adsorbent, J. Mol. Liq. 213 (2016) 162–172, https://doi.org/10.1016/j.molliq.2015.11.011.
[59] Fao. 2022b. Food and Agriculture Organization - Database [Online]. Available: http://www.fao.org/faostat/ [Accessed 02. June 2022].
[60] J.I. Morán, V.A. Alvarez, V.P. Cyras, A. Vázquez, Extraction of cellulose and preparation of nanocellulose from sisal fibers, Cellulose 15 (2007) 149–159, https://doi.org/10.1007/s10570-007-9145-9.
[61] Z. Movasaghi, B. Yan, C. Niu, Adsorption of ciprofloxacin from water by pretreated oat hulls: equilibrium, kinetic, and thermodynamic studies, Ind. Crops Prod. 127 (2019) 237–250, https://doi.org/10.1016/j.indcrop.2018.10.051.
[62] P. Rajkumar, M. Somasundaram, Non-isothermal conversion of wheat husk and low-density polyethylene for energy dense fuel production, Biomass Convers. Biorefinery 12 (2020) 5695–5705, https://doi.org/10.1007/s13399-020-00951-3.
[63] D.W. Silva, M.V. Scatolino, N.R.T. Do Prado, R.F. Mendes, L.M. Mendes, Addition of different proportions of castor husk and pine wood in particleboards, Waste Biomass Valoriz. 9 (2016) 139–145, https://doi.org/10.1007/s12649-016-9742-7.
[64] L.Z. Zhi, L. Te Chuan, M.A. Selimin, N. Pagan, J.A. Halip, Physical properties of rice husk-pine wood particleboard, J. Sustain. Mater. Process. Manag. 1 (2021) 8–16.